# 3D MORPHOLOGICAL IMPACT MODELLING OF OFFSHORE WIND FARMS USING LES AND HPC

Yue Yin[1], Elizabeth Christie[1], Ming Li[1], Charles Moulinec[2] and David R. Emerson[2]

A model based on TELEMAC 3D using Large Eddy Simulation has been developed to simulate of complex flows and sediment transport around offshore wind farm foundations. The model was tested against available laboratory experimental data with satisfactory agreement. The model results reveal that with fine resolution, using Large Eddy Simulation allows to capture the turbulence eddy shedding behind the structure better than using conventional RANS models. Application of the model to the Burbo Bank OWF in Liverpool Bay, in North West England helps capturing the strong 3D structures across the depth, which can have considerable influence on sediment suspension and transport around the structure, particularly for fine sediments.

*Keywords: offshore wind farms; TELEMAC3D; large eddy simulation*

## INTRODUTION

With recent fast development of offshore wind farms (OWF), it is important to understand any impacts they might have on large scale coastal hydrodynamics and morphodynamics. A recent study by Christie et al (2012) has shown that it is possible to include the OWF structure directly in the oceanographic model with high grid resolution around each individual monopile. Unfortunately, the conventional Reynolds Averaged Navier-Stokes (RANS) turbulence closures, such as k-ε and k-ω, become inefficient to describe turbulence generation and dissipation immediately adjacent to the monopile as well as the large scale wake tailing behind the whole OWF. To satisfy stability criteria, the computational time step has also to be small, which limits the model's capability for long term simulations. The present research therefore intends to substitute the RANS turbulence closure with Large Eddy Simulation (LES) and investigate its performance and accuracy for far field modelling.

The aim of this paper is to demonstrate the capability of the coastal morphodynamic model TELEMAC3D (Hervouet, 2007; http://www.opentelemac.org) to predict the flow and sediment transport around offshore wind farm foundations. Prior to this investigation, TELEMAC3D is first validated at laboratory scale by simulating the flow around a cylinder lying on the bottom of a channel. Results are compared to the experimental data obtained by Roulund et al (2005), using their configuration.

## NUMERICAL METHOD

### Governing equations

An open source hydrodynamic suite, TELEMAC, is used to simulate the hydrodynamics impact of offshore wind farms. The 3D module, TELEMAC3D is a three-dimensional computational code solving either the hydrostatic or non-hydrostatic equations. In this work the hydrostatic approximation is used both at laboratory scale and field scale. The code solves the three-dimensional hydrodynamic equations based on the following assumptions (courtesy of Hervouet (2007)):

1. Three-dimensional Navier-Stokes equations with a free surface changing in time,
2. Negligible variation of density in the conservation of mass equation (incompressible fluid),
3. Pressure-hydrostatic assumption (that assumption results in that the pressure at a given depth is the sum of the air pressure at the fluid surface plus the weight of the overlying water body),
4. Boussinesq approximation for the momentum (the density variations are not taken into account in the gravity term)

Due to these assumptions, the three-dimensional equations being solved are:

$$\frac{\partial U}{\partial x}+\frac{\partial V}{\partial y}+\frac{\partial W}{\partial z}=0 \tag{1}$$

$$\frac{\partial U}{\partial t}+U\frac{\partial U}{\partial x}+V\frac{\partial U}{\partial y}+W\frac{\partial U}{\partial z}=-g\frac{\partial Z_s}{\partial x}+\nu\Delta U+F_x \tag{2}$$

$$\frac{\partial V}{\partial t}+U\frac{\partial V}{\partial x}+V\frac{\partial V}{\partial y}+W\frac{\partial V}{\partial z}=-g\frac{\partial Z_s}{\partial y}+\nu\Delta V+F_y \tag{3}$$

$$p=p_{atm}+\rho_0 g(Z_s-z)+\rho_0 g\int_Z^{Z_s}\frac{\Delta\rho}{\rho_0}dZ \tag{4}$$

[1] School of Engineering, University of Liverpool, L69 3GQ, Liverpool, U.K.
[2] Science and Technology Facilities Council, Daresbury Laboratory, WA4 4AD, U.K.

where *U*, *V* and *W* are three-dimensional components of velocity; $Z_s$ is the free surface elevation and $F_x$, $F_y$ are source terms. Pressure is calculated in Eq. 4 where $\rho_0$ and $\Delta\rho$ are reference density and variation of density respectively.

Based on these assumptions, TELEMAC3D model can be split up in three fractional steps:

-The first step consists in finding out the advected velocity components by only solving the advection terms in the momentum equations.

-The second step computes, from the advected velocities, the new velocity components taking into account the diffusion terms and the source term in the momentum equations. These two solutions enable to obtain an intermediate velocity field.

-The third step is provided for computing the water depth from the vertical integration of the continuity equation and the momentum equations only including the pressure-continuity terms (all the other terms have already been taken into account in the earlier two steps). The resulting two-dimensional equations (analogous to the Shallow Water equations without diffusion, advection and source terms) are written as:

$$\frac{\partial h}{\partial t} + \frac{\partial (uh)}{\partial x} + \frac{\partial (vh)}{\partial y} = 0 \tag{5}$$

$$\frac{\partial u}{\partial t} = -g \frac{\partial Z_s}{\partial x} \tag{6}$$

$$\frac{\partial v}{\partial t} = -g \frac{\partial Z_s}{\partial y} \tag{7}$$

The *u* and *v* in lower case denote the two-dimensional variables of the vertically integrated velocity. These two-dimensional equations are solved by the libraries in the TELEMAC-2D code and enable to obtain the vertically averaged velocity and the water depth. The water depth makes it possible to re-compute the elevations of the various mesh points and then those of the free surface. Lastly, the computation of the *U* and *V* velocities is simply achieved through a combination of the equations linking the velocities. Finally, the vertical velocity *W* is computed from the continuity equation.

**Turbulence model**

In this study, the LES closure based on the Smagorinski sub-grid scheme has been selected as the turbulence model for the horizontal directions. Smagorinski (1963)'s idea is to add to the molecular viscosity a turbulent viscosity deduced from a mixing length model. This mixing length corresponds to the size of the vortices smaller than that of the mesh size.

$$v_t = {C_s}^2 \Delta^2 \sqrt{2 D_{ij} D_{ij}} \tag{8}$$

where $C_s$ is a dimensionless coefficient to be calibrated and $\Delta$ is the mesh size derived in 2D or 3D from the surface or from the volume of the element. The value of $C_s$ is set to 0.1 for canal condition.

A mixing-length model is used as a turbulence model for the vertical direction. This model, proposed by Prandtl (1925) gives the value of the viscosity coefficient as:

$$v_t = {L_m}^2 \sqrt{2 D_{ij} D_{ij}} \tag{9}$$

where $D_{ij}$ is the strain rate tensor of average motion, with:

$$D_{ij} = \frac{1}{2}\left(\frac{\partial \overline{U_\iota}}{\partial x_j} + \frac{\partial \overline{U_J}}{\partial x_i}\right) \tag{10}$$

$L_m$ is the "mixing length" parameter equal to *kz* at a distance *z* from the bottom, and *k*=0.41 (von Karman constant).

It is expected that the seabed boundary and the structure wall will influence the results. In particularly, the important parameters are the shear velocity, defined by $\tau = -\rho(U^*)^2$ and the dimensionless distance to the wall $y^+ = \frac{yU^*}{v}$, where $y$ is the distance to the wall. $z^+$ is defined as $z^+ = \frac{zU^*}{v}$ at the bottom. In this study, the mean value of $y^+$ is 240 and of $z^+$ is 130, which stats that boundary condition are in the logarithmic range. In this condition, the turbulent viscosity is then written as $v_t = kU^*y$. The velocity profile takes the following form:

For hydraulically smooth flow:

$$\frac{U}{U^*} = \frac{1}{k} ln\left(\frac{yU^*}{v}\right) + 0.52 \tag{11}$$

For hydraulically rough flow:

$$\frac{U}{U^*} = \frac{1}{k} ln\left(\frac{33y}{k_s}\right) = \frac{1}{k} ln\left(\frac{y}{k_s}\right) + 0.85 \quad (12)$$

where $k$ is the von Karman constant and $k_s$ is the roughness size.

## MODEL VALIDATION

TELEMAC3D is widely used by the coastal engineering community. Accurately modeling turbulence with these coastal models is often proven to be challenging. Therefore the accuracy of the coastal model in the simulation of such complex flow condition is always one of the main users' focuses. In order to obtain reasonable results from simulations, numerical model is validated against laboratory experiment, involving steady flow around a circular cylinder as described in Roulund et al. (2005).

Following the experimental setup in Roulund et al. (2005), the simulation domain as shown in Figure 1 is set to be 50 m long by 4 m wide. The bed is assumed to be flat with a constant depth of 0.54 m. A cylinder with diameter of 0.53 m is placed at 13 m downstream of the inlet. The 3D mesh of the simulation domain contains 282,740 elements in 2D and has 20 unevenly distributed horizontal layers.

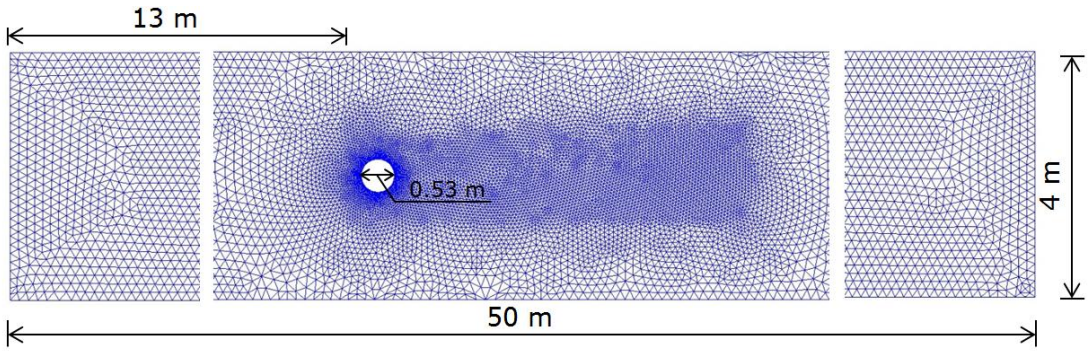


**Figure 1. Geometry of the computed domain.**

Two conditions from the experiment are used to test the model, one for a smooth bed and another one for a rough bed. In both cases, the simulations are carried out at Re=1.7×10$^5$, with inlet velocity U = 0.326 m/s. The time step of 0.01 s is chosen to keep the maximum Courant number below 0.8.

In order to compare the measured mean flow velocities obtained in the experiment, the computed instantaneous velocities are averaged over 10,000 time steps after the initial settle down period in the numerical model.

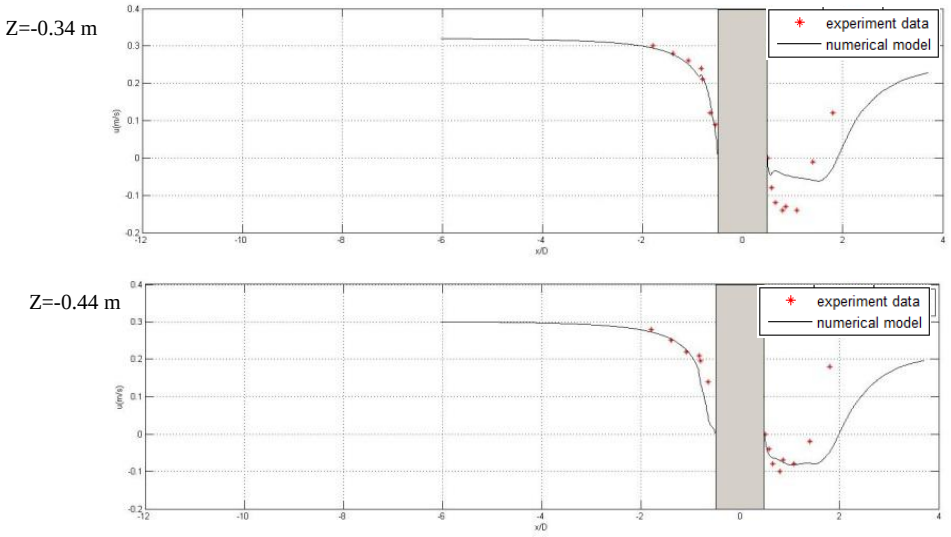

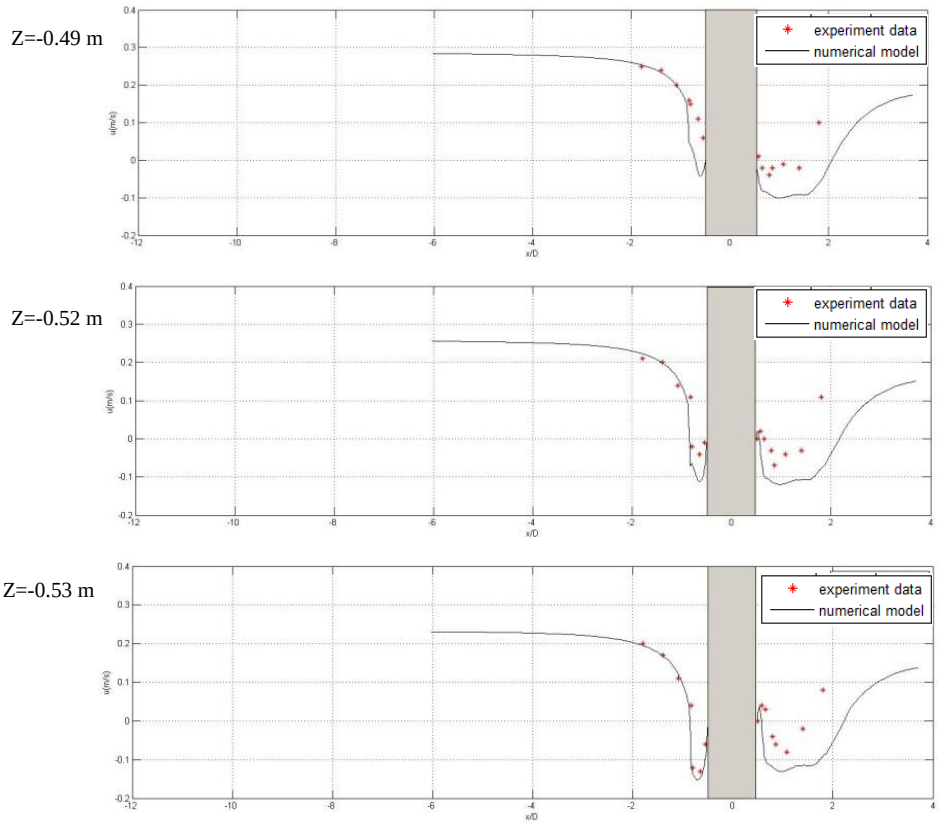


**Figure 2. Mean horizontal velocity in the streamwise plane of symmetry at different distances from the bed using a smooth rigid bed condition**

Figure 2 compares the computed mean horizontal velocity distributions with experimental data at different layers for the smooth bed condition. Overall, the velocity profile in front of cylinder shows a better agreement in comparison with the experimental data. Small deviations can be observed in the area which is close to the structure. At the layer Z=-0.44 m, the flow velocity decreases slightly faster than for the experimental data. At the layer Z=-0.49 m, the minimum flow speed in the experiment is around 0 m/s. However in the numerical model, velocities reduce to negative values first and then recover to 0 m/s at the wall of the cylinder. At the layers Z= -0.52 m and -0.53 m, negative velocities are both found in numerical model and experimental data. In the wake part, at the layer Z= -0.34 m the minimum flow velocity of the numerical model does not reach to the peak observed in the experimental data. At the layer Z= -0.44 m the minimum flow velocity of numerical model is close to the peak of experimental data but a small difference can still be found. At the layers Z= -0.49 m, -0.52 m and -0.53 m, the minimum flow velocity of the numerical model is over- predicted. Although in the wake part the length of the wake is over-estimated, the tendency of the flow recovery behind the structure still shows a reasonable agreement. At the layer Z = = -0.34 m, -0.44 m and -0.49 m, both numerical model and experimental data show a down and up trend. At the layer Z = -0.52 m and 0.53 m, experimental data shows a significant feature that flow velocity slightly increases before reducing to negative values, then recovers to outlet speed, which is represented by the numerical model.

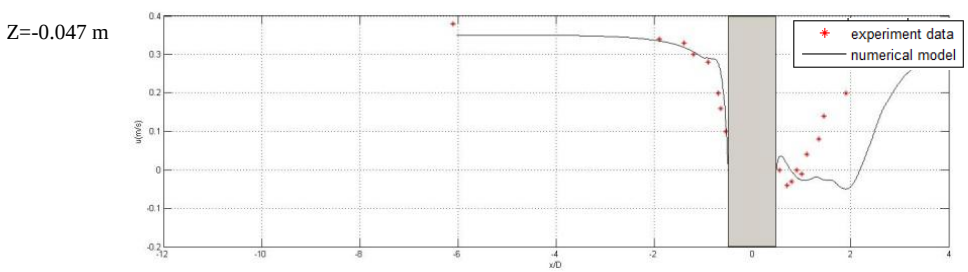

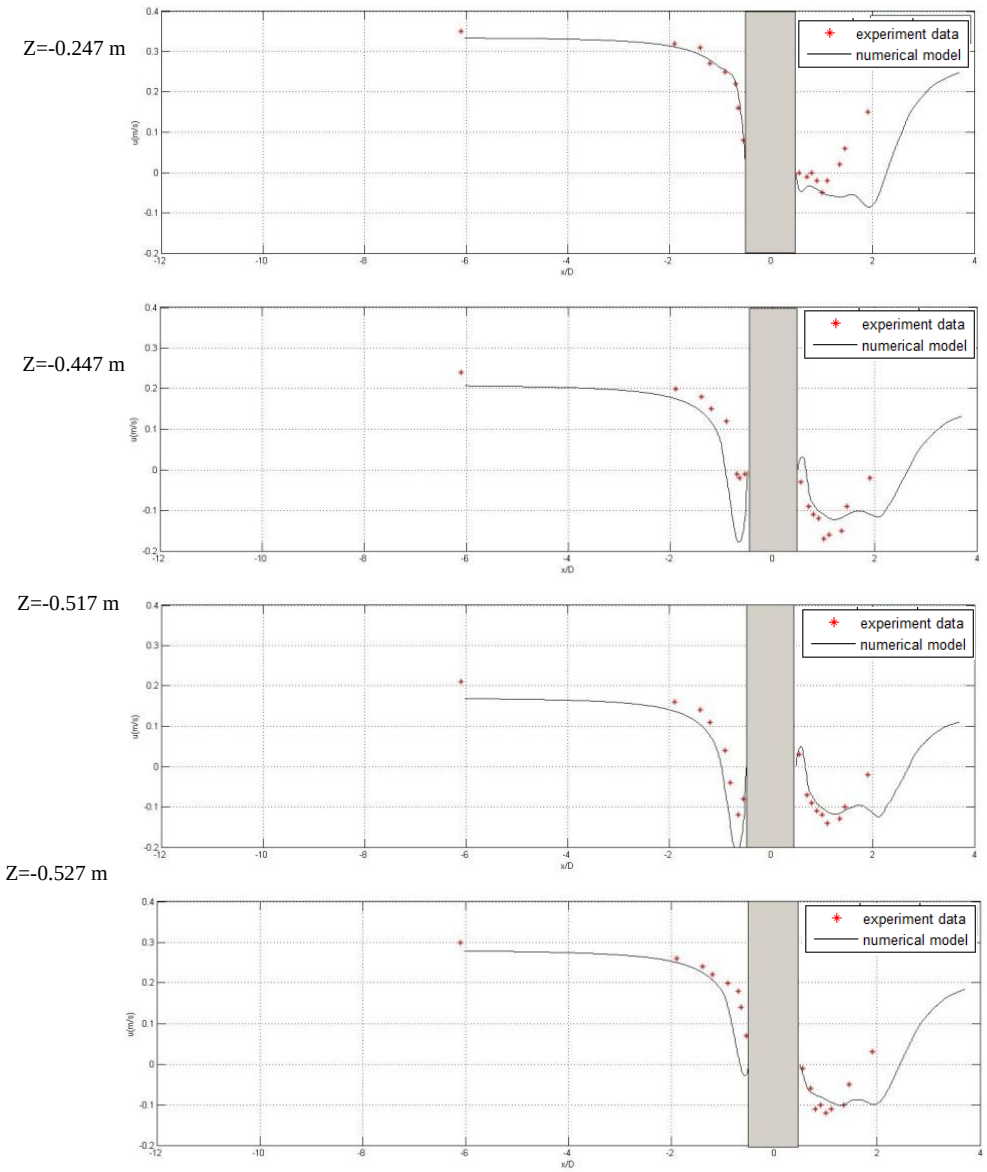


**Figure 3. Mean horizontal velocity in the plane of symmetry at different distances from the bed using a rough rigid bed condition**

Similarly, Figure 3 shows the mean horizontal velocity distributions obtained for a rough bed test using the same mesh as for the previous case. The velocity profile in front of the cylinder shows a good agreement with the experimental data, which is also observed for the smooth bed test case. However in layers Z = -0.517 m and -0.527 m, the measured velocities are slightly under-estimated by the numerical model. In the wake part, the minimum mean velocities are closed to the peak of the experimental data, but the wake length is clearly over-predicted. In the numerical models, it takes longer for the flow to recover to the flow. The difference in wake length between numerical model and experimental data reduces from the surface layer to the bottom layer and a much closer agreement can be found at Z = -0.527m level.

## MODEL APPLICATION

The model is then used for far field simulations at Liverpool Bay, Eastern Irish Sea where three OWFs exist, namely Burbo Bank, North Hoyle and Rhyl Flats, consisting of 25, 30 and 25 monopile turbines respectively. The fine mesh is shown in Figure 4 where the details of the grid around the structures have been highlighted. The mesh contains 323,830 elements in 2D and has 15 horizontal layers. The cell size varies from 0.4 m on cylinder walls to 5500 m at the open boundary. The monopile

has a typical diameter of 4-5m. The average distance between each turbine structure is about 350 m to 540 m.

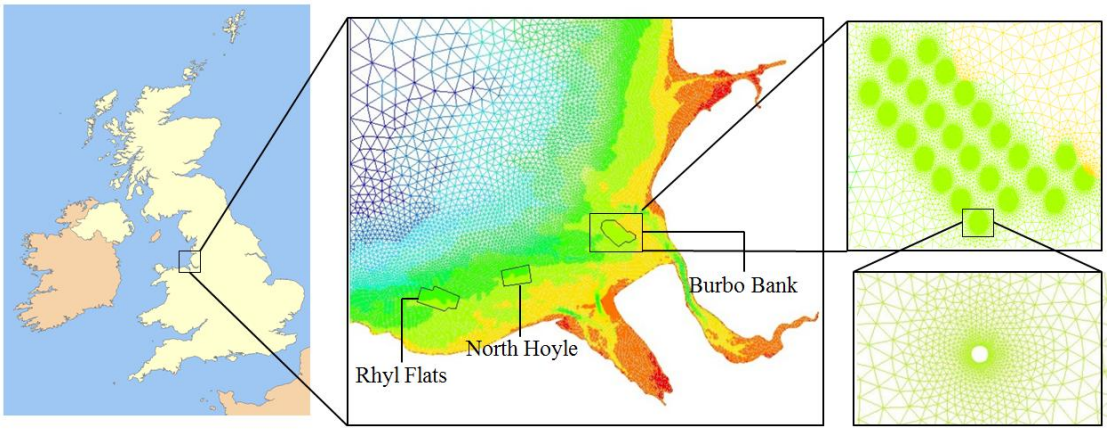


**Figure 4. Mesh of Liverpool Bay**

Boundary conditions used include offshore open boundary with the tidal water level or riverine discharge specified and solid wall shoreline boundaries. The model is driven by scaled representative tides calculated by the Tidal Model Driver (Egbert & Erofeeva, 2002) for 7 tidal constituents (M2, S2, N2, K2, P1, O1, K2). Riverine discharge is also included as a model input with annual mean flow rate specified at the boundaries of the Dee, Mersey, Douglas and Ribble estuaries as 33.70m3/s, 37.22 m3/s, 4.16 m3/s, 33.04 m3/s respectively. Bottom friction is calculated by the Chézy formula with a Chézy coefficient of 24. Sediment transport is modeled with the Meyer-Peter bed load transport formula with a single sediment size class of diameter 0.23mm, and the morphology is updated with the Exner equation.

## Results

Both the hydrodynamics and morphological impacts of OWF are investigated by numerical simulations. For the hydrodynamics study, the model is run over a full spring-neap tidal cycle (over 30 days) to catch the peak flow. For the morphological study, TELEMAC3D is coupled with SISYPHE the sediment transport module and run for less than 7 days due to time step limitation.

Figure 5 shows the computed depth averaged velocity around OWF during a peak flow spring tide. Remarkable decrease in the depth averaged velocity can be found in the wake of each monopile foundation. At spring tide, the wake tail behind certain structures at Burbo Bank is over 200 meters long. However this distance is still shorter than the average distance between each cylinder. Consequently, it is difficult to see the flow interaction between adjacent piles.

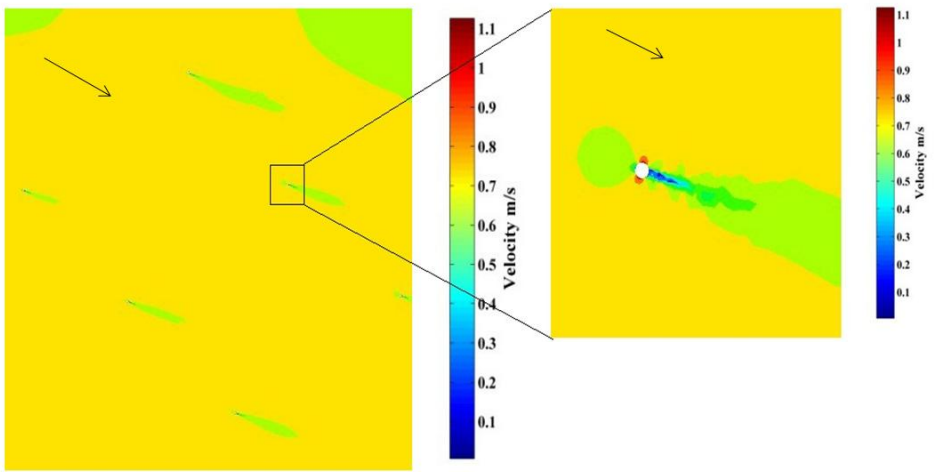


**Figure 5. Depth averaged velocity over part of the Burbo Bank OWF (highlighted) obtained from a 3-D model simulation**

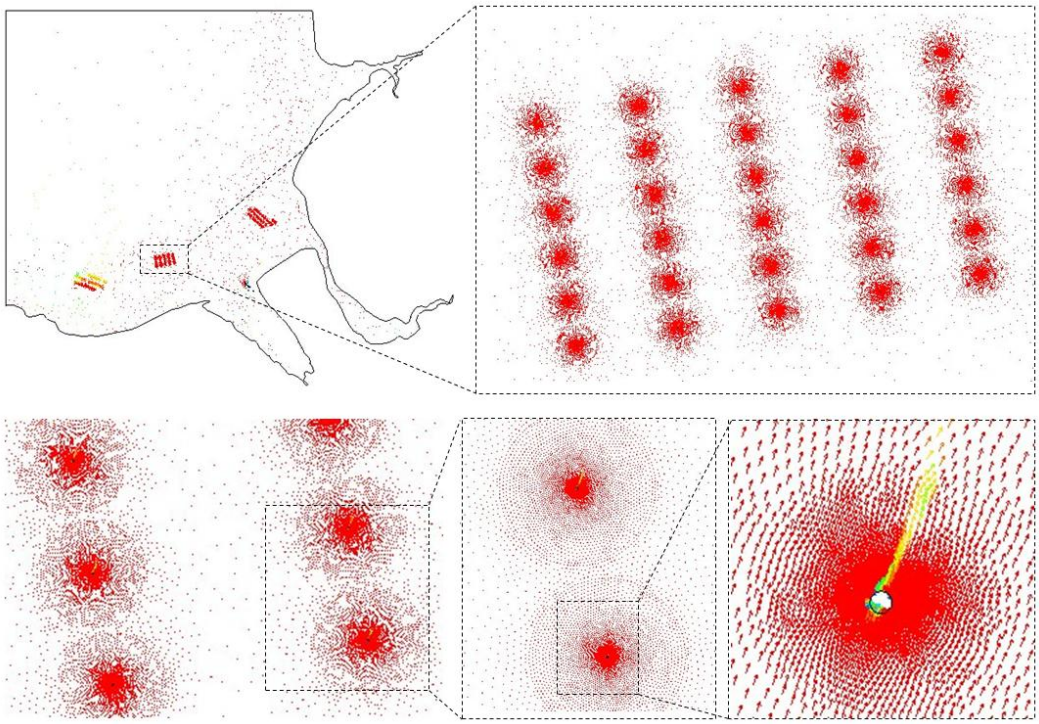

**Figure 6. Flow profile displayed by "Arrows" style**

Figure 6 presents the distribution of flow vectors in the whole test domain. The flow pattern is represented by "arrow" style, in which the length and color of arrows represent the magnitude of the flow velocity and the direction of arrows is consistent with flow direction. As can be observed in this figure, the interaction between adjacent pile wakes is weak. The flow impact of the whole wind turbine farm cannot be represented so far.

Due to the element-size dependence of the LES turbulence closure, the model is tested with two different meshes. Figure 7 compares the flow pattern for different mesh at the same time period and the difference can be clearly seen. Figure 7(a) is the result for the mesh of 323,830 elements and Figure 7(b) is that for the mesh of 1,295,230 elements. The mesh in Figure 7 (b) is refined from previous mesh by mesh multiplication. Although noticeable wake tail behind piles can be found in both results, the length of the wake for the refined mesh is much longer than the one for the initial mesh. Flow interaction between two piles can be found in Figure 7(b).

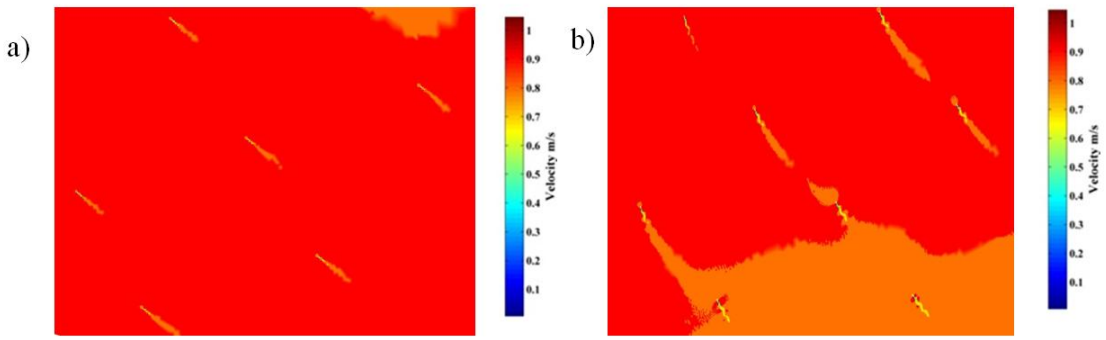


**Figure 7. Depth averaged velocity over part of the Burbo Bank wind farm with different size of mesh. a) 323,830 2D elements; b) 1,295,320 2D elements**

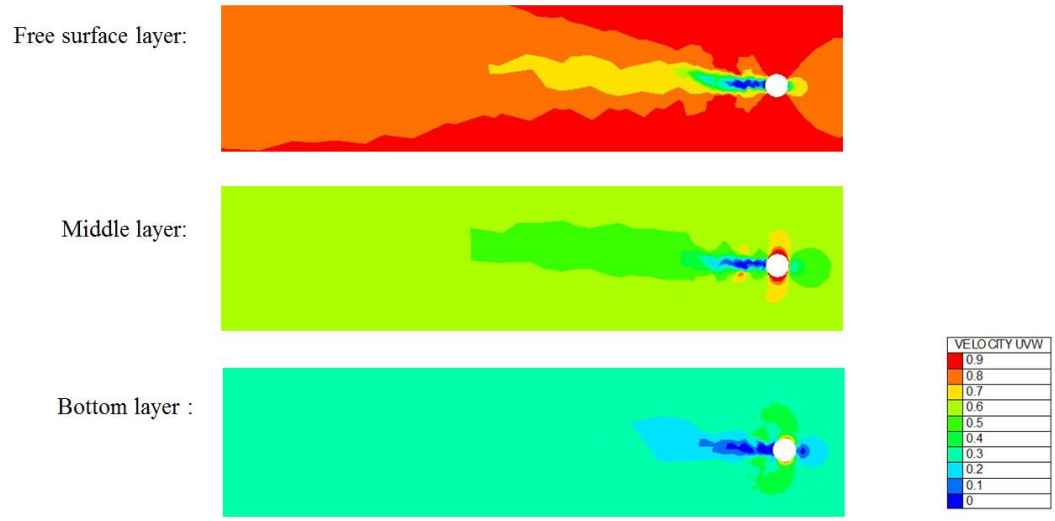


**Figure 8. Velocity distribution at one monopile turbine at the North Hoyle wind farm for the 3-D model simulation at different layers**

Figure 8 shows the distribution of the magnitude of the instantaneous velocity around a turbine at free surface layer, middle layer and bottom layer separately. In all three layers, similar flow patterns can be found with a decrease in velocity in the wake of the pile and flow acceleration at the side of the pile. However it is obvious that the wake illustrated in the free surface layer is much longer than the wake in the bottom layer. The wake in the middle layer is twice as long as for the bottom layer wake. With the increase of water depth, velocity accelerations at both sides of the pile play more significantly roles in hydrodynamics.

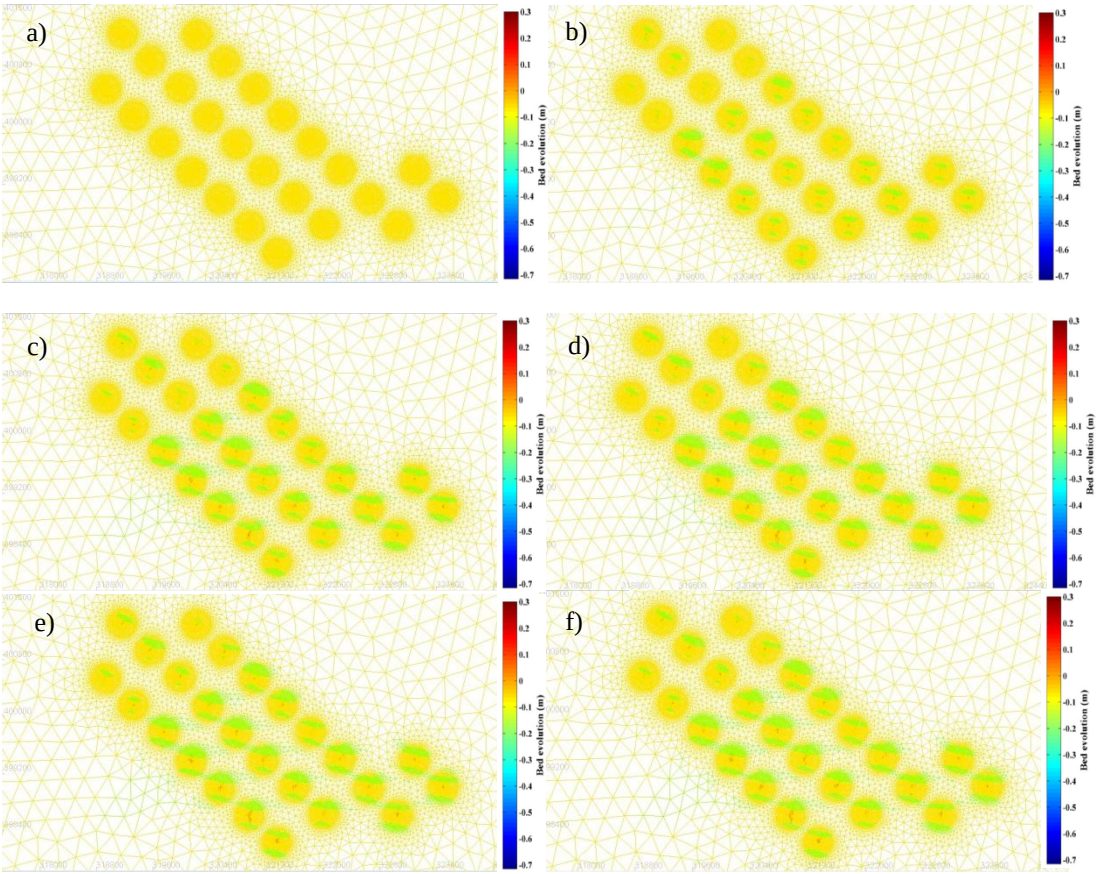


**Figure 9. Bed evolution around OWF of Burbo Bank**

In Figure 9, the computed bed evolution is presented around the OWF of Burbo Bank over a 5 days period. Figure 9(a) shows the initial state of the seabed and the following figures illustrate the seabed evolution for each day. Comparing the six figures, scour on the seabed develops rapidly in the first three days and then begin to remain stable. Marked scour area can be found in both sides of each monopole turbine which is parallel to the flow direction. However the areas of deposition cannot be observed, which suggests that the sediment being eroded from the structure site and subsequently transported away from the site leads to the net erosion at the OWF.

## CONCLUSIONS

In this study, TELEMAC3D is used to simulate the flow around a circular cylinder at laboratory scale and model both hydrodynamics and morphological impact of OWF at large scale. At laboratory scale, LES gives a reasonable agreement with the experimental data for a flow around a cylinder. Although TELEMAC3D cannot reach the same accuracy as a CFD solver would, it can still catch and represent the flow's key features. For most engineering propose, the accuracy of TELEMAC3D is acceptable.

At the prototype scale, the model is tested at the OWF at Liverpool Bay in which the OWF foundation structures are represented by the mesh directly with high resolution around each individual structure. The initial model test suggests the tidal flow has complex 3D structures across the depth and the weak behind the individual turbine foundation is clearly seen in the results. However the interaction between adjacent pile wakes is not obvious, but can be found in very high resolution configurations.

## ACKNOWLEDGMENTS

The current study is supported by EPSRC and EDF Energy through an iCASE studentship. The technical supports from Computing Services of the University of Liverpool and from the Hartree Centre are also greatly appreciated.

## REFERENCES

Christie E., M. Li, C. Moulinec. 2012. Comparison of 2d and 3d large scale morphological modeling of offshore wind farms using HPC. *International Conference on Coastal Engineering 2012 Proceedings.* World Scientifics, Santander pp sediment.42

Hervouet J-M. 2007. Hydrodynamics of free surface flows: modelling with the finite element method, *Wiley*

The TELEMAC system. <http://www.opentelemac.org>

Roulund, A., B.M. Sumer, J. Fredsøe, J. Michelsen. 2005. Numerical and experimental investigation of flow and scour around a circular pile. *Journal of Fluid Mechanics*, 534, pp. 351-401

Smagorinski, J. 1963 General circulation experiments with the primitive equations. I. The basic experiment. Monthly Weather Review, 91,99-164

Prandtl, L., 1925. Über die ausgebidete Turbulenz. Zeitschrift für augewandte Mathematik und Mechanik. 5, pp. 136-139